Motion Mode Analysis of a Variable-DOF Parallel Mechanism via Higher-Order Kinematic Analysis

Andreas Müller and Xianwen Kong

Abstract This paper presents the motion mode analysis of a variable-DOF parallel mechanism (VDPMs) with four RRRRR legs using a higher-order analysis. It is shown that this VDPM has four different motion modes, where the platform performs 3-DOF planar motions, 3-DOF motions with zero torsion, 3-DOF spatial translations, and 2-DOF motions in a plane, respectively. The presented result enriches the types of overconstrained and variable-DOF (also kinematotropic) mechanisms, and has practical value for synthesis of VDPM in particular.

1 Introduction

Multi-mode parallel mechanisms (PMs) [20] are a novel class of reconfigurable mechanisms that can switch between different operation modes without the need for disconnection and reassembly. Current research on multi-mode PMs mainly focuses on multi-mode PMs [9] in which all the motion modes have the same degree of freedom (DOF). The number of variable-DOF parallel mechanisms (VDPMs) (or kinematotropic PMs) [18, 4, 6] proposed so far is very limited. It has been found that several PMs may have extra motion modes [5, 8, 3, 14, 15] in addition to the expected motion modes. Although the PMs in [3, 14, 15] can be counted as VDPMs, the motions in the extra motion modes are complicated to describe. This may hinder the application of the PMs in these extra motion modes. Therefore, VDPMs, especially those whose motion modes can be readily described, are still not well explored.

A. Müller
Johannes Kepler University, Linz, Austria
e-mail: a.mueller@jku.at

X. Kong
Heriot-Watt University, Edinburgh, UK
e-mail: X.Kong@hw.ac.uk

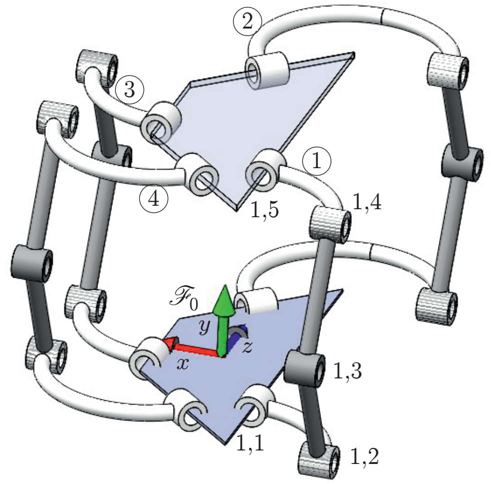

Fig. 1 The VDPM in the analyzed reference configuration. Each of the four legs (encircled number) comprises 5 revolute joints (numbered with $1,\ldots,5$).

In this paper, we will present a novel 4-RRRRR PM VDPM (see Fig. 1) whose motion modes can be intuitively described. As will be revealed using the higher order analysis [11, 12] later in this paper, the proposed VDPM possesses four operation modes where the platform performs 3 DOF planar motions, 3 DOF spatial translations, 3 DOF motions with zero torsion, and a 2 DOF motion in a plane, respectively. Moreover the actual instantaneous motions in each mode are revealed.

2 Description of the Variable-DOF Parallel Mechanism

The variable-DOF 4-RRRRR PM is composed of four RRRRR legs $L = 1,\ldots,4$. Each leg comprises five revolute joints numbered 1 to 5 from the base to platform. Joints 2, 3 and 4 in each leg have parallel axes forming a planar kinematic linkage. Let $\cdot^i_j$ denote joint j in leg i. In total the PM comprises $n = 20$ joints. The PM topology is represented by the directed topological graph $\vec{\Gamma}$ in Fig. 2. A PM with simple L legs possesses $\gamma = L - 1$ fundamental cycles (FC) [10], see also [13] for the case of complex legs. The 4-RRRRR PM has $L = 4$ limbs, thus $\gamma = 3$ FC. The corresponding $\gamma = 3$ loop constraints are the basis for kinematic modeling and analysis.

The above VDPM was derived from a 3-legged 3-DOF PM capable of both planar and spatial translational motion modes [7] by adding an extra leg and fine-tuning the link parameters through a trial-and-error process.

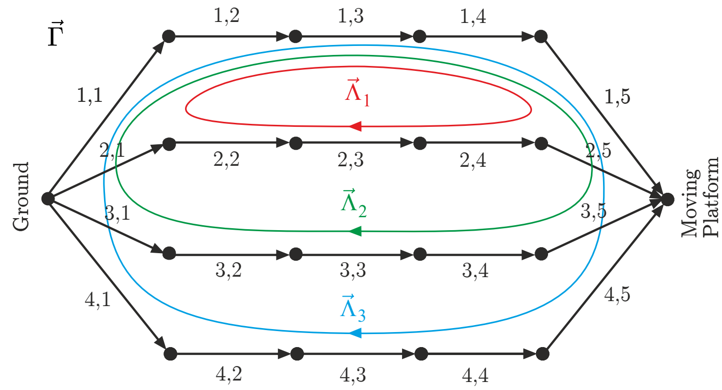

Fig. 2 Directed topological graph $\vec{\Gamma}$ and the $\gamma = 3$ FCs Λ_l for the PM in Fig 1. The edge labeled with l, i represents joint i of leg l.

3 Joint Screw System in Reference Configuration

Denote with $\mathbf{p}_i^l \in \mathbb{R}^3$ the vector to a point on the axis of joint i in limb $l = 1, \ldots, 4$, and with $\mathbf{e}_i^l \in \mathbb{R}^3$ a unit vector along the joint axis. Denote with $\mathbf{q} \in \mathbb{V}^n$ the vector of joint angles. To the configuration shown in Fig. 1 is assigned $\mathbf{q} = \mathbf{0}$. In this configuration, the position vectors and unit vectors are

$$\mathbf{p}_1^1 = \begin{bmatrix} -3 \\ -1 \\ 0 \end{bmatrix}, \ \mathbf{p}_2^1 = \begin{bmatrix} -3 \\ -1 \\ 0 \end{bmatrix}, \ \mathbf{p}_3^1 = \begin{bmatrix} -4 \\ -1 \\ 2 \end{bmatrix}, \ \mathbf{p}_4^1 = \begin{bmatrix} -3 \\ -1 \\ 4 \end{bmatrix}, \ \mathbf{p}_5^1 = \begin{bmatrix} -3 \\ -1 \\ 4 \end{bmatrix} \tag{1}$$

$$\mathbf{p}_1^2 = \mathbf{p}_2^2 = \begin{bmatrix} -1 \\ 1 \\ 0 \end{bmatrix}, \mathbf{p}_3^2 = \begin{bmatrix} -2 \\ 1 \\ 2 \end{bmatrix}, \ \mathbf{p}_4^2 = \mathbf{p}_5^2 = \begin{bmatrix} -1 \\ 1 \\ 4 \end{bmatrix}, \mathbf{p}_1^3 = \mathbf{p}_2^3 = \begin{bmatrix} 1 \\ 1 \\ 0 \end{bmatrix}, \mathbf{p}_3^3 = \begin{bmatrix} 2 \\ 1 \\ 2 \end{bmatrix}$$

$$\mathbf{p}_4^3 = \mathbf{p}_5^3 = \begin{bmatrix} 1 \\ 1 \\ 4 \end{bmatrix}, \mathbf{p}_1^4 = \mathbf{p}_2^4 = \begin{bmatrix} 3 \\ -1 \\ 0 \end{bmatrix}, \mathbf{p}_3^4 = \begin{bmatrix} 4 \\ -1 \\ 2 \end{bmatrix}, \mathbf{p}_4^4 = \mathbf{p}_5^4 = \begin{bmatrix} 3 \\ -1 \\ 4 \end{bmatrix}$$

$$\mathbf{e}_1^1 = \mathbf{e}_5^1 = \mathbf{e}_1^3 = \mathbf{e}_5^3 = [1,0,0]^T, \quad \mathbf{e}_1^2 = \mathbf{e}_5^2 = \tfrac{1}{2}[\sqrt{2}, \sqrt{2}, 0]^T \tag{2}$$

$$\mathbf{e}_1^4 = \mathbf{e}_5^4 = \tfrac{1}{2}[-\sqrt{2}, \sqrt{2}, 0]^T, \quad \mathbf{e}_2^l = \mathbf{e}_3^l = \mathbf{e}_4^l = [0,1,0]^T, l = 1, \ldots, 4.$$

All vectors are measured in the reference frame $\mathcal{F}_0$ indicated in Fig. 1. The instantaneous screw coordinate vector of revolute joint i in limb l at $\mathbf{q} = \mathbf{0}$ is $\mathbf{S}_i^l = \begin{bmatrix} \mathbf{e}_i^l \\ \mathbf{e}_i^l \times \mathbf{p}_i^l \end{bmatrix}$. The assignment of $\mathbf{q} = \mathbf{0}$ to the investigated configuration is just for convenience. Any arbitrary configuration $\mathbf{q}$ can be used.

4 Finite Mobility Analysis

At $\mathbf{q} = \mathbf{0}$, the overall constraint Jacobian of the $\gamma = 3$ loop constraints according to the FC as in Fig. 2 is

$$\mathbf{J}\,(\mathbf{0}) = \begin{bmatrix} \mathbf{S}_1^1 & \mathbf{S}_2 & \mathbf{S}_3^1 & \mathbf{S}_4^1 & \mathbf{S}_5^1 & -\mathbf{S}_1^2 & -\mathbf{S}_2^2 & -\mathbf{S}_3^2 & -\mathbf{S}_4^2 & \mathbf{S}_5^2 & \mathbf{0} & \mathbf{0} & \mathbf{0} & \mathbf{0} & \mathbf{0} & \mathbf{0} & \mathbf{0} & \mathbf{0} & \mathbf{0} & \mathbf{0} \\ \mathbf{S}_1^1 & \mathbf{S}_2^1 & \mathbf{S}_3^1 & \mathbf{S}_4^1 & \mathbf{S}_5^{11} & \mathbf{0} & \mathbf{0} & \mathbf{0} & \mathbf{0} & \mathbf{0} & -\mathbf{S}_1^3 & -\mathbf{S}_2^3 & -\mathbf{S}_3^3 & -\mathbf{S}_4^3 & -\mathbf{S}_5^3 & \mathbf{0} & \mathbf{0} & \mathbf{0} & \mathbf{0} & \mathbf{0} \\ \mathbf{S}_1^1 & \mathbf{S}_2^1 & \mathbf{S}_3^1 & \mathbf{S}_4^1 & \mathbf{S}_5^1 & \mathbf{0} & \mathbf{0} & \mathbf{0} & \mathbf{0} & \mathbf{0} & \mathbf{0} & \mathbf{0} & \mathbf{0} & \mathbf{0} & \mathbf{0} & -\mathbf{S}_1^4 & -\mathbf{S}_2^4 & -\mathbf{S}_3^4 & -\mathbf{S}_4^4 & -\mathbf{S}_5^4 \end{bmatrix}. \tag{3}$$

In this configuration, the Jacobian has rank $\mathbf{J}\,(\mathbf{0}) = 15$. The 1st-order DOF of the PM is thus $\delta_{\text{diff}}\,(\mathbf{0}) = 20 - 15 = 5$.

The finite mobility and motion modes are established using the higher-order local analysis reported in [11, 12]. The basic concept behind the higher-order local analysis is to construct a low-dimensional algebraic variety that locally approximates the analytic c-space variety V. In regular configurations $\mathbf{q} \in V$, this is the tangent space to V at $\mathbf{q}$. In a general configuration this is a cone. The kinematic tangent cone is defined by the tangents to smooth finite arcs in V (smooth motions) through $\mathbf{q} \in V$ as $C_{\mathbf{q}}^{\mathrm{K}}V := \{\dot{\sigma}|\sigma \in C_{\mathbf{q}}\} \subset \mathbb{R}^n$, where $C_{\mathbf{q}}$ is the class of smooth arcs (analytic germs) in V through $\mathbf{q} \in V$. It is constructed successively as $C_{\mathbf{q}}^{\mathrm{K}}V = K_{\mathbf{q}}^{\kappa} \subseteq \ldots \subseteq K_{\mathbf{q}}^3 \subseteq K_{\mathbf{q}}^2 \subseteq K_{\mathbf{q}}^1$, where the ith-order cone is defined as

$$\begin{aligned} K_{\mathbf{q}}^i := \{\mathbf{x}|\exists \mathbf{y}, \mathbf{z}, \ldots \in \mathbb{R}^{20} : H_l^{(1)}(\mathbf{q}, \mathbf{x}) = \mathbf{0}, H_l^{(2)}(\mathbf{q}, \mathbf{x}, \mathbf{y}) = \mathbf{0}, H_l^{(3)}(\mathbf{q}, \mathbf{x}, \mathbf{y}, \mathbf{z}) = \mathbf{0}, \ldots \\ \ldots, H_l^{(i)}(\mathbf{q}, \mathbf{x}, \mathbf{y}, \mathbf{z}, \ldots) = \mathbf{0}, l = 1, 2, 3\}. \end{aligned} \tag{4}$$

The ith-order constraint map for the FC l is defined as $H_l^{(1)}(\mathbf{q}, \dot{\mathbf{q}}) := \mathbf{J}_l(\mathbf{q})\dot{\mathbf{q}}$ and $H_l^{(i)}(\mathbf{q}, \dot{\mathbf{q}}, \ldots, \mathbf{q}^{(i)}) := \frac{d^{i-1}}{dt^{i-1}} H_l^{(1)}(\mathbf{q}, \dot{\mathbf{q}})$ so that the ith-order constraint is

$$H_l^{(i)}(\mathbf{q}, \dot{\mathbf{q}}, \ldots, \mathbf{q}^{(i)}) = \mathbf{0}. \tag{5}$$

The constraint maps are determined algebraically from the joint screw coordinate vectors by simple screw products [12]. The first-order cone $K_{\mathbf{q}}^1$ is a vector space in $\mathbf{x}$, which is the tangent space if $\mathbf{q}$ is a regular point of V, i.e. V is a manifold.

The analysis yields $C_{\mathbf{q}}^{\mathrm{K}}V = K_{\mathbf{q}}^4 \subset K_{\mathbf{q}}^3 = K_{\mathbf{q}}^2 \subset K_{\mathbf{q}}^1$, where the first-order cone is

$$\begin{aligned} K_{\mathbf{0}}^1 = \{\, & \mathbf{x} \in \mathbb{R}^{20} | x_1^1 = r, x_2^1 = s, x_3^1 = t, x_4^1 = u, x_5^1 = v, x_1^2 = \sqrt{2}r, x_2^2 = -t - u + v, \\ & x_4^2 = r - s - t, x_3^2 = -2r + 2s + 3t + 2u - 2v, x_5^2 = \sqrt{2}v, x_1^3 = r, \\ & x_2^3 = -r + 3s + 3t + 2u - v, x_3^3 = 2r - 4s - 5t - 4u + 2v, \\ & x_4^3 = -r + 2s + 3t + 3u - v, x_5^3 = v, x_1^4 = -\sqrt{2}r, x_2^4 = r + 4s + 4t + 3u, \\ & x_3^4 = -6s - 7t - 6u, x_4^4 = 3s + 4t + 4u + v, x_5^4 = -\sqrt{2}v; r, s, t, u, v \in \mathbb{R} \,\}. \end{aligned}$$

The 2nd-order cone is the union $K_{\mathbf{0}}^2 = K_{\mathbf{0}}^{2(1)} \cup K_{\mathbf{0}}^{2(2)}$, with $\dim K_{\mathbf{0}}^{2(1)} = \dim K_{\mathbf{0}}^{2(2)} = 3$,

$$
\begin{aligned}
K_{\mathbf{0}}^{2(1)} = \{\, \mathbf{x} \in \mathbb{R}^{20} | & x_1^1 = r, x_3^1 = s, x_4^1 = t, x_5^1 = r, x_1^2 = \sqrt{2}r, x_2^2 = r - s - t, \\
& x_3^2 = -4r + 2x_2^1 + 3s + 2t, x_4^2 = r - x_2^1 - s, x_5^2 = \sqrt{2}r, x_1^3 = r, \\
& x_2^3 = -2r + 3x_2^1 + 3s + 2t, x_3^3 = 4r - 4x_2^1 - 5s - 4t, \\
& x_4^3 = -2r + 2x_2^1 + 3(s+t), x_5^3 = r, x_1^4 = -\sqrt{2}r, x_2^4 = r + 4x_2^1 + 4s + 3t, \\
& x_3^4 = -6x_2^1 - 7s - 6t, x_4^4 = r + 3x_2^1 + 4(s+t), x_5^4 = -\sqrt{2}r, \\
& x_1^4 = -\sqrt{2}r, x_2^4 = r + s + t, x_3^4 = -t, x_4^4 = -x_1^1 - s, x_5^4 = \sqrt{2}r;\ r, s, t \in \mathbb{R} \,\} \\
K_{\mathbf{0}}^{2(2)} = \{\, \mathbf{x} \in \mathbb{R}^{20} | & x_1^1 = r, x_2^1 = s, x_3^1 = t, x_4^1 = -s - t, x_5^1 = -r, x_1^2 = \sqrt{2}r, \\
& x_2^2 = s - r, x_3^2 = t, x_4^2 = r - s - t, x_5^2 = -\sqrt{2}r, x_1^3 = r, x_2^3 = s + t, \\
& x_3^3 = -t, x_4^3 = -s, x_5^3 = -r, ;\ r, s, t \in \mathbb{R} \,\}.
\end{aligned}
$$

The 3rd- and 2nd-order cones are equal, $K_{\mathbf{0}}^3 = K_{\mathbf{0}}^2$. Finally the 4th-order cone is $K_{\mathbf{0}}^4 = K_{\mathbf{0}}^{4(1)} \cup K_{\mathbf{0}}^{4(2)} \cup K_{\mathbf{0}}^{4(3)} \cup K_{\mathbf{0}}^{4(4)}$, with $\dim K_{\mathbf{0}}^{4(1)} = \dim K_{\mathbf{0}}^{4(2)} = \dim K_{\mathbf{0}}^{4(3)} = 3, \dim K_{\mathbf{0}}^{4(4)} = 2$,

$$
\begin{aligned}
K_{\mathbf{0}}^{4(1)} = \{\, \mathbf{x} \in \mathbb{R}^{20} | & x_1^1 = 0, x_5^1 = 0, x_1^2 = 0, x_5^3 = 0, x_1^4 = 0, x_5^2 = 0, x_1^3 = 0, x_5^4 = 0, \\
& x_2^1 = r, x_3^1 = s, x_4^1 = t, x_2^2 = -s - t, x_3^2 = 2r + 3s + 2t, x_4^2 = -r - s, \\
& x_2^3 = 3r + 3s + 2t, x_3^3 = -4r - 5s - 4t, x_4^3 = 2r + 3(s+t), \\
& x_2^4 = 4r + 4s + 3t, x_3^4 = -6r - 7s - 6t, x_4^4 = 3r + 4(s+t);\ r, s, t \in \mathbb{R} \,\} \\
K_{\mathbf{0}}^{4(2)} = \{\, \mathbf{x} \in \mathbb{R}^{20} | & x_1^1 = r, x_2^1 = s, x_3^1 = t, x_4^1 = s, x_5^1 = r, x_1^2 = \sqrt{2}r, x_2^2 = r - s - t, \\
& x_3^2 = -4r + 4s + 3t, x_4^2 = r - s - t, x_5^2 = \sqrt{2}r, x_1^3 = r, x_2^3 = -2r + 5s + 3t, \\
& x_3^3 = 4r - 8s - 5t, x_4^3 = -2r + 5s + 3t, x_5^3 = r, x_1^4 = -\sqrt{2}r, x_2^4 = r + 7s + 4t, \\
& x_3^4 = -12s - 7t, x_4^4 = r + 7s + 4t, x_5^4 = -\sqrt{2}r;\ r, s, t \in \mathbb{R} \,\} \\
K_{\mathbf{0}}^{4(3)} = \{\, \mathbf{x} \in \mathbb{R}^{20} | & x_1^1 = r, x_2^1 = s, x_3^1 = t, x_4^1 = -s - t, x_5^1 = -r, x_1^2 = \sqrt{2}r, x_2^2 = -r + s, \\
& x_3^2 = t, x_4^2 = r - s - t, x_5^2 = -\sqrt{2}r, x_1^3 = r, x_2^3 = s + t, x_3^3 = -t, x_4^3 = -s, x_5^3 = -r, \\
& x_1^4 = -\sqrt{2}r, x_2^4 = r + s + t, x_3^4 = -t, x_4^4 = -r - s, x_5^4 = \sqrt{2}r;\ r, s, t \in \mathbb{R} \,\} \\
K_{\mathbf{0}}^{4(4)} = \{\, \mathbf{x} \in \mathbb{R}^{20} | & x_1^1 = r, x_3^1 = s, x_2^1 = -\tfrac{s}{2}, x_4^1 = -\tfrac{s}{2}, x_5^1 = r, x_1^2 = \sqrt{2}r, x_2^2 = r - \tfrac{s}{2}, \\
& x_3^2 = -4r + s, x_4^2 = r - \tfrac{s}{2}, x_5^2 = \sqrt{2}r, x_1^3 = r, x_2^3 = \tfrac{1}{2}(-4r + s), x_3^3 = 4r - s, \\
& x_4^3 = \tfrac{1}{2}(-4r + s), x_5^3 = r, x_1^4 = -\sqrt{2}r, x_2^4 = r + \tfrac{s}{2}, x_3^4 = -s, \\
& x_4^4 = r + \tfrac{s}{2}, x_5^4 = -\sqrt{2}r;\ r, s, t \in \mathbb{R} \,\}
\end{aligned}
$$

The tangent cone is the union of four vector spaces, each locally describing the finite motions on a motion manifold passing through $\mathbf{q} = \mathbf{0}$. The corresponding motion modes are shown in Fig. 3. The vector spaces $K_{\mathbf{0}}^{4(i)}, i = 1, 2, 3$ are three dimensional and $K_{\mathbf{0}}^{4(4)}$ is two-dimensional, thus the PM possess 3 DOF and 2 DOF, respectively. In conclusion the PM can enter four motion modes from the investigated configuration $\mathbf{q} = \mathbf{0}$. The latter is a singularity of V (c-space singularity), which implies that it is a kinematic singularity, i.e. the rank of $\mathbf{J}$ is higher than 5 in any neighborhood of $\mathbf{q} = \mathbf{0}$. It can be shown that the rank of $\mathbf{J}$ is 17 in motion modes 1, 2, and 3, and the rank is 18 in motion mode 2. This analysis proceeds by analyzing the tangent cone to motions of certain rank [11, 12].

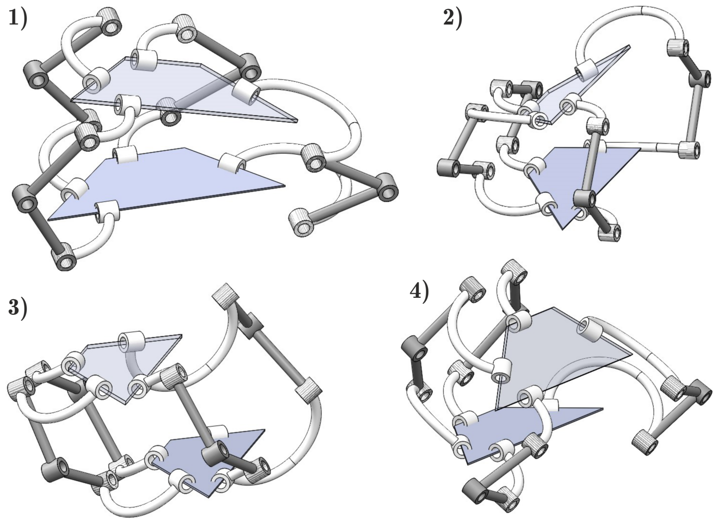

Fig. 3 The four motion modes the VDPM can enter from the singular configuration in Fig. 1: 1) planar motions, 2) 3-DOF zero torsion, 3) spatial translations, 4) 2-DOF motion in the y-z plane.

5 Motion Mode Analysis

The important information for the PM design are motion modes of the platform. The instantaneous platform motion is described by the platform twist $\mathbf{V}_{\mathrm{p}} = \left[\begin{smallmatrix}\omega_{\mathrm{p}}\\ \mathbf{v}_{\mathrm{p}}\end{smallmatrix}\right]$, expressed in $\mathcal{F}_0$. It is determined by the joint screws as

$$\mathbf{V}_{\mathrm{p}} = \left[\mathbf{S}_1^l\ \mathbf{S}_2^l\ \mathbf{S}_3^l\ \mathbf{S}_4^l\ \mathbf{S}_5^l\right] [x_1^l, x_2^l, x_3^l, x_4^l, x_5^l]^T \tag{6}$$

for any $l = 1, \ldots, 4$. For the four vector spaces defining the motion modes this yields

$$\begin{aligned}
\mathbf{V}_{\mathrm{p}}^{(1)} &= \left[0, x_2 + x_3 + x_4, 0, -2x_3 - 4x_4, 0, -3x_2 - 4x_3 - 3x_4\right]^T \\
\mathbf{V}_{\mathrm{p}}^{(2)} &= \left[2x_1, 2x_2 + x_3, 0, -4x_2 - 2x_3, 4x_1, 2x_1 - 6x_2 - 4x_3\right]^T \\
\mathbf{V}_{\mathrm{p}}^{(3)} &= \left[0, 0, 0, 4x_2 + 2x_3, -4x_1, -x_3\right]^T, \mathbf{V}_{\mathrm{p}}^{(4)} = \left[2x_1, 0, 0, 0, 4x_1, 2x_1 - x_3\right]^T
\end{aligned} \tag{7}$$

The first describes 3-DOF platform motions in the x-z plane of $\mathcal{F}_0$ [7], the second a 3-DOF motion with zero torsion [2], the third describes a 3-DOF pure spatial translation [7], and the fourth mode is a 2-DOF motion composed of 1-dimensional translation in the y-z plane of $\mathcal{F}_0$ with an independent rotation about the plane normal.

6 Conclusions

A four-mode VDPM has been proposed. This VDPM has three typical 3-DOF modes and one 2-DOF motion along a plane. The higher-order analysis provides an efficient approach to identify the motion modes of a VDPM at a reference configuration. There are other configuration that allow for motion mode change. The local analysis must be carried out for each of them separately.

This work enriches the types of VDPMs. The type synthesis [6], reconfiguration analysis [5, 8, 17, 16] of VDPMs and measures for switching a VDPM between different operation modes [1, 19] remain open issues. Potential application of these VDPMs also deserve further investigation.

Acknowledgements The first author (AM) acknowledges support by the LCM-K2 Center within the framework of the Austrian COMET-K2 program, and by the Austrian Science Fund (FWF) [I 4452-N]. The second author (XK) would like to thank the Engineering and Physical Sciences Research Council (EPSRC), United Kingdom, for the support under grant No. EP/T024844/1.

References

1. Chablat, D., Kong, X., Zhang, C.: Kinematics, workspace, and singularity analysis of a parallel robot with five operation modes. ASME Journal of Mechanisms and Robotics **10**(3), 035,001 (2018)
2. Chen, Z., Kong, X., Zhao, C., Huang, Z.: Type synthesis of 3-RSR equivalent 2R1T parallel mechanisms based on screw theory. Mechanism and Machine Theory **211**, 106,032 (2025)
3. Coste, M., Mady Demdah, K.: Extra modes of operation and self-motions in manipulators designed for schoenflies motion. Journal of Mechanisms and Robotics **7**(4), 041,020 (2015)
4. Fanghella, P., Galleti, C., Gianotti, E.: Parallel robots that change their group of motion. In: Advances in Robot Kinematics, pp. 49–56. Springer (2006)
5. Husty, M.L., Schröcker, H.P.: Kinematics and algebraic geometry. In: J.M. McCarthy (ed.) 21st Century Kinematics, pp. 85–123. Springer London, London (2013)
6. Kong, X.: Type synthesis of variable degree-of-freedom parallel manipulators with both planar and 3T1R operation modes. In: Proceedings of ASME 2012 International Design Engineering Technical Conferences & Computers and Information in Engineering Conference, pp. DETC2012–70,621. ASME (2012)
7. Kong, X.: Type synthesis of 3-DOF parallel manipulators with both a planar operation mode and a spatial translational operation mode. Journal of Mechanisms and Robotics **5**(4) (2013)
8. Kong, X.: Reconfiguration analysis of a 3-DOF parallel mechanism using euler parameter quaternions and algebraic geometry method. Mechanism and Machine Theory **74**, 188–201 (2014)
9. Kong, X., He, X., Kostalas, T.: Type synthesis of a novel class of one-DOF multi-mode parallel mechanisms. Journal of Mechanisms and Robotics **17**(4), 044,504 (2024)
10. Mueller, A.: Dynamics of parallel manipulators with hybrid complex limbs –modular modeling and parallel computing. Mechanism and Machine Theory **167**, 104,549 (2022)
11. Müller, A.: Local investigation of mobility and singularities of linkages. In: A. Müller, Z. Zlatanov (eds.) Singular Configurations of Mechanisms and Manipulators, CISM 589. Springer (2019)
12. Müller, A.: An overview of formulae for the higher-order kinematics of lower-pair chains with applications in robotics and mechanism theory. Mech. Mach. Theory **142** (2019)

13. Müller, A.: A constraint embedding approach for dynamics modeling of parallel kinematic manipulators with hybrid limbs. Robotics and Autonomous Systems **155**, 104,187 (2022)
14. Nurahmi, L., Caro, S., Wenger, P., Schadlbauer, J., Husty, M.: Reconfiguration analysis of a 4-RUU parallel manipulator. Mechanism and Machine Theory **96**, 269–289 (2016). Reconfigurable mechanisms
15. Nurahmi, L., Putrayudanto, P., Wei, G., Agrawal, S.K.: Geometric constraint-based reconfiguration and self-motions of a four-cru parallel mechanism. ASME Journal of Mechanisms and Robotics **13**(2), 021,017 (2021)
16. Tang, Z., Feng, H., Dai, J.S.: Computation of kinematic paths and bifurcation points for multi-degree-of-freedom mechanisms with singular value decomposition. Mechanism and Machine Theory **213**, 106,047 (2025)
17. Wampler, C.W., Sommese, A.J.: Numerical algebraic geometry and algebraic kinematics. Acta Numerica **20**, 469567 (2011)
18. Wohlhart, K.: Kinematotropic linkages. In: Recent Advances in Robot Kinematics, pp. 359–368. Springer (1996)
19. Ye, W., Hu, L., Li, Q.: Kinematic analysis and dimension optimization of a new reconfigurable parallel mechanism with 1R2T and 2R1T operation modes. ASME Journal of Mechanisms and Robotics **14**(6), 060,914 (2022)
20. Yu, J., Liu, K., Kong, X.: State of the art of multi-mode mechanisms. Jixie Gongcheng Xuebao/Journal of Mechanical Engineering **56**(19), 14–27 (2020)